

Supporting Information for

**Efficient synthesis strategy of near-zero volume change
material for all-solid-state batteries operable under minimal
stack pressure**

Teppei Ohno,¹ Yosuke Ugata,^{1,2} and Naoaki Yabuuchi*,^{1,2}

¹Department of Chemistry and Life Science, Yokohama National University, 79-5

Tokiwadai, Hodogaya-ku, Yokohama 240-8501, Japan

²Advanced Chemical Energy Research Center (ACERC), Institute of Advanced

Sciences, Yokohama National University, 79-5 Tokiwadai, Hodogaya-ku, Yokohama

240-8501, Japan

***CORRESPONDING AUTHOR**

E-mail: yabuuchi-naoaki-pw@ynu.ac.jp (N.Y.)

Experimental

Synthesis of materials

$\text{Li}_{8/7}\text{Ti}_{2/7}\text{V}_{4/7}\text{O}_2$ (LTVO) was prepared by a solid-state reaction from a mixture of 3 mol% excess Li_2CO_3 (98.5%, Kanto Kagaku), anatase type TiO_2 (98.5%, Wako Pure Chemical Industries), and V_2O_3 (98%, Sigma Aldrich). The precursors were mixed by wet ball milling at 300 rpm with ethanol for 5 h, and the mixtures were pressed into pellets after drying in air. These pellets were calcinated at various temperatures with different durations in an Ar atmosphere. A heating ramp-up rate of 10 deg./min was used with different target temperatures (650–900 °C) under an Ar flow rate of 50 mL/min. Optimized LTVO were prepared by ball milling using a planetary ball mill (PULVERISETTE 7; FRITSCH) with a zirconia container and balls at 450 rpm for 6 h in an argon atmosphere. LiVO_2 was also synthesized via a solid-state reaction. For the synthesis of LiVO_2 , 3 mol% excess Li_2CO_3 (98.5%, Kanto Kagaku) and V_2O_3 (98%, Sigma Aldrich) were mixed by wet ball milling at 300 rpm with ethanol for 5 h, and the mixtures were pressed into pellets after drying in air. The pellet was calcinated at 900 °C for 12 h in Ar. The calcinated samples were subsequently ball-milled at 450 rpm for 6 h.

LTVO was also prepared via a solution-based method using a mixture of 3 mol% excess CH_3COOLi (98%, Wako Pure Chemical Industries), $\text{V}(\text{C}_5\text{H}_7\text{O}_2)_3$ (97%, Sigma Aldrich), and $\text{TiO}(\text{C}_5\text{H}_7\text{O}_2)_2$ (Ti assay = 17–21 wt%, Kanto Kagaku), all dissolved in ethylene glycol (99.5%, Kishida chemical). The solution was stirred at 150 °C for 24 h to form a homogeneous dark-green solution. The solution was heated at 250 °C to obtain Li-Ti-V-O mixtures, and then the mixtures were calcinated at 400 °C for 3 h and subsequently at 600–900 °C for 3 h in an Ar atmosphere.

Electrochemical characterization

The optimized LTVO was mixed with acetylene black (AB) (LTVO:AB = 90:10 wt%) by hand mixing in an agate mortar and pestle for 15 min to prepare a carbon composite. The composite positive electrode consisting of 76.5 wt% active material, 13.5 wt% AB, and 10 wt% poly(vinylidene fluoride) (PVdF, KF 1100, Kureha Co. Ltd.) was cast on an Al foil used as a current collector. The composite electrodes were dried at room temperature for 2 h and then at 120 °C for 2 h under vacuum. Metallic lithium (Honjo Metal) was used as a negative electrode. 1 M LiPF₆ dissolved in ethylene carbonate (EC)/ dimethyl carbonate (DMC) mixture (30:70 vol%) or highly concentrated electrolyte solution (HCE), 5.5 M LiN(SO₂F)₂ (LiFSA) in DMC, purchased from Kishida Chemical was used as an electrolyte solution. A microporous polyolefin membrane (Celgard 2500, Celgard) and aramid-coated polyolefin film^{1, 2} (LIELSORT[®], Teijin Limited) were used as separators for low-concentration electrolyte and HCE, respectively. Electrode performance of the samples was examined in two-electrode electrochemical cells (TJ-AC, Tomcell Japan). The cells were cycled in the voltage range of 1.2–4.3 V at a rate of 10 mA g⁻¹ or 30 mA g⁻¹ at room temperature.

Surface morphology and composition analysis

Surface morphology of the samples was observed using a scanning electron microscope (SEM, JCM-6000, JEOL) with an acceleration voltage of 15 kV. Elemental distributions were observed using SEM with an energy dispersive X-ray spectrometer (EDX, JSM-IT200, JEOL). The Brunauer–Emmett–Teller (BET) specific surface area was measured at 77 K using a micromeritics surface area and porosity analyzer

(BELSORP MINI X; Microtrac MRB). Phase purity and crystal structures of the obtained samples were studied using an X-ray diffractometer (D2 PHASER, Bruker) equipped with a one-dimensional X-ray detector using Cu K α radiation ($\lambda = 1.5413 \text{ \AA}$) generated at 300 W (30 kV and 10 mA). *In-situ* XRD patterns were collected using an electrochemical cell equipped with a Be window and X-ray diffractometer (Bruker, D8 Advance) using Cu K α radiation generated at 1600 W (40 kV and 40 mA) with a Ni filter. The surface of the active materials was analyzed using an X-ray photoelectron spectrometer (Quantera-SXM, ULVAC-PHI).

Preparation of solid electrolyte sheets

Li_{5.5}PS_{4.5}Cl_{1.5}^{3,4} (LPSCl; NEI corp.) was used as a solid electrolyte. LPSCl was heat-treated at 500 °C 2 h to remove surface impurities before use. Heat-treated LPSCl and poly(vinylidene fluoride-co-hexafluoropropylene) copolymer⁵ (PVdF-HFP, Daikin Industries) were dispersed in a mixed solvent of benzyl acetate⁶ (BA) (99%, battery grade, Kishida Chemical) and butyl butylate^{5,6} (BB) (99%, battery grade, Kishida Chemical) at 1000 rpm for 15 min to obtain a LPSCl slurry (LPSCl:PVdF-HFP = 93:7 wt%). The resulting slurry was coated on a silicone-coated polyethylene terephthalate film using a doctor blade. The sheet was dried at room temperature overnight and further 2 h at 100 °C under vacuum. The dried sheet was then punched into a disk with a diameter of 15 mm. The thickness of the prepared SE sheet was ~100 μm . All the preparation procedures for LPSCl sheets were conducted in an Ar-filled glove box.

Fabrication of all-solid-state batteries

LTVO, LPSCl, and vapor grown carbon fiber (VGCF) were mixed in a weight ratio

of 47:45:5 wt% to prepare the composite electrode. The precursors were placed into a zirconia pot with ZrO₂ balls and milled at 150 rpm for 2 h by using a planetary ball mill. The ball-milled powders were then mixed with PVdF-HFP in BB/BA mixed solvent to obtain an electrode slurry. The slurry was coated on an Al foil as current collector and subsequently dried under vacuum at room temperature overnight. The composite electrode was punched into a disk with a diameter of 10 mm and then vacuum dried at 100 °C for 2 h. The composition of the composite electrode was LTVO:LPSCl:VGCF:PVdF-HFP = 47:45:5:3 in wt%. The cross-sectional morphologies of the composite electrodes were observed with a field emission scanning electron microscope (FE-SEM; SU8010, Hitachi High-Technologies) coupled with energy-dispersive X-ray spectroscopy (EDX). Cross-sectional specimens of the electrodes were prepared using an ion-milling system (IM4000 II, Hitachi High-Technologies).

Electrochemical performance of LTVO/LPSCl composite electrode was examined in electrochemical cells with the same configuration as the cell with liquid electrolytes under low stack pressure (< 0.5 MPa). The stack pressure inside the cell was measured using pressure-indicating films (ultra super low pressure film, Fujifilm Prescale). The composite electrode, LPSCl sheet, and Li_xIn alloy⁷ ($x = \sim 0.5$, $\varnothing = 12$ mm) negative electrode were assembled in a two-electrode cell (TJ-AC; Tomcell Japan). To densify the composite electrode and enhance the interfacial contact within composite electrode and across electrode/electrolyte sheet interface, cold isostatic press (CIP) treatment was conducted.⁸ The composite electrode was first pressurized at 480 MPa for 10 min by CIP (HPV-50C20-S, Sugino Machine). After CIP treatment, the pressed composite electrode was assembled with the electrolyte sheet and Li_xIn alloy. The assembled cell was further pressurized again at 480 MPa for 10 min by CIP.

Supporting Table and Figures

Table S1. Electrochemical performance of reported all-solid-state batteries with layered-oxide positive electrode materials and sulfide-based solid electrolytes under various stack pressures.

positive electrode material	stack pressure / MPa	initial discharge capacity / mA h g ⁻¹	capacity retention (100 th) / %	current density / mA g ⁻¹	temperature / °C	solid electrolyte	Ref.
Li_{8/7}Ti_{2/7}V_{4/7}O₂	0.5	198	99	50	50	Li_{5.5}PS_{4.5}Cl_{1.5}	this work
LiNiO ₂	2	188	92	36	60	Li ₆ PS ₅ Cl	[48]
LiNi _{0.8} Co _{0.1} Mn _{0.1} O ₂	2	155	86	28	25	Li ₆ PS ₅ Cl	[49]
LiNi _{0.80} Co _{0.15} Al _{0.05} O ₂	5	150	81	28	R.T.	Li ₆ PS ₅ Cl	[44]
LiNi _{0.8} Co _{0.1} Mn _{0.1} O ₂	25	153	80	54	30	Li ₁₀ SnP ₂ S ₁₂	[46]
LiNi _{0.6} Co _{0.2} Mn _{0.2} O ₂	100	120	100	106	25	Li ₆ PS ₅ Cl	[47]
LiNi _{0.83} Co _{0.11} Mn _{0.06} O ₂	100	152	95	95	30	Li ₆ PS ₅ Cl/Li ₃ InCl ₆	[45]
LiNiO ₂	150	203	90	36	35	Li ₆ PS ₅ Cl	[48]

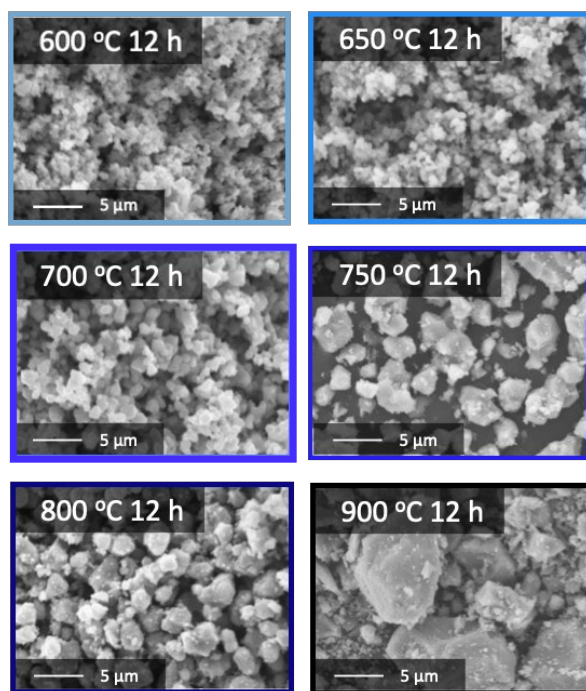


Figure S1. SEM images of LTVO calcinated at different temperatures.

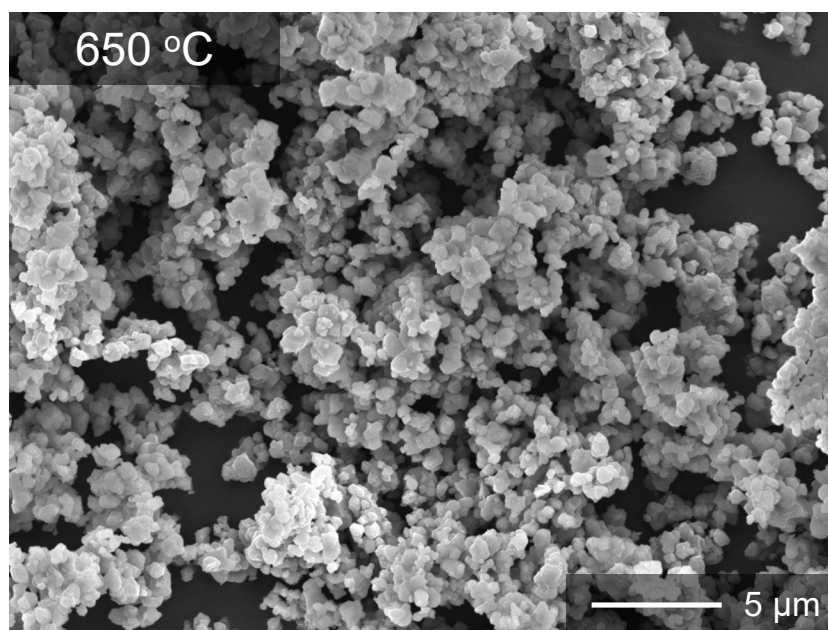
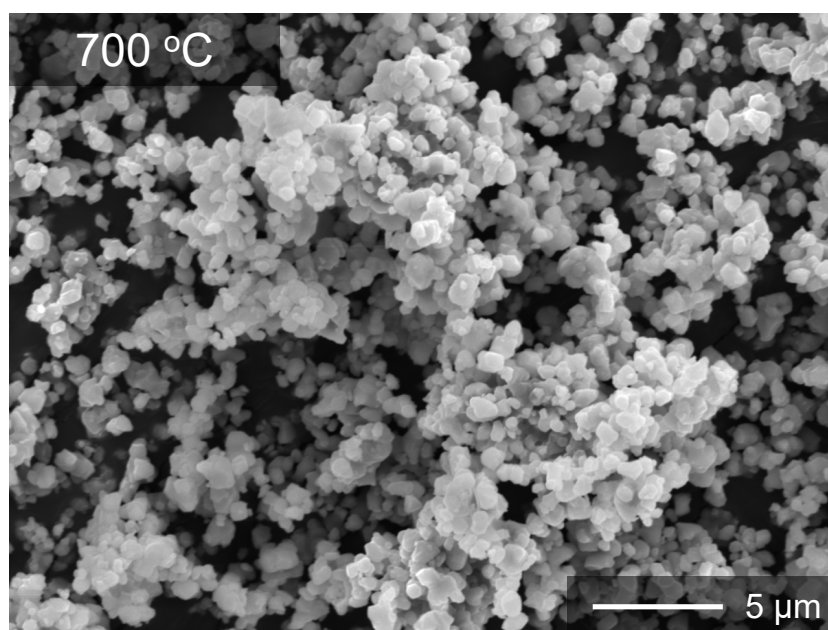


Figure S2. SEM images of LTVO calcinated at 700 and 650 °C.

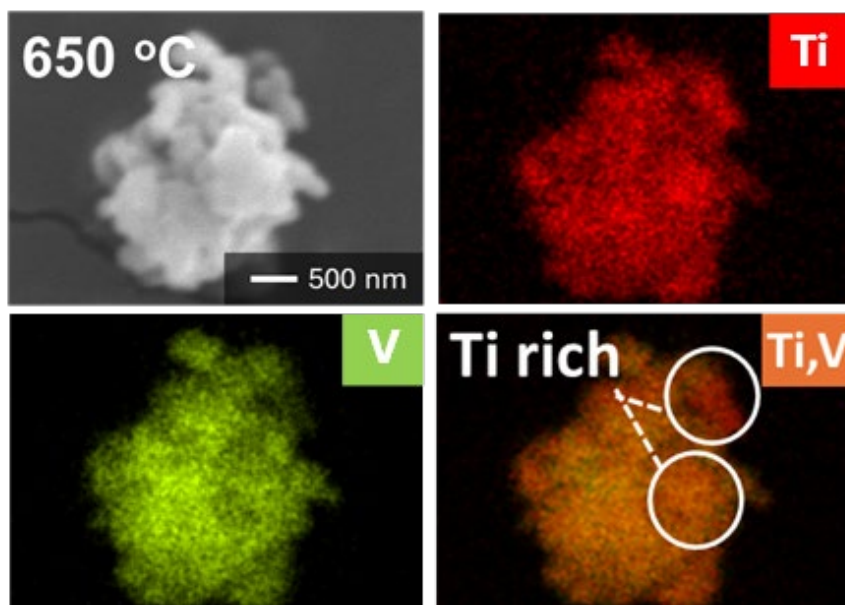


Figure S3. SEM images and EDX maps of LTVO calcinated at 650 °C.

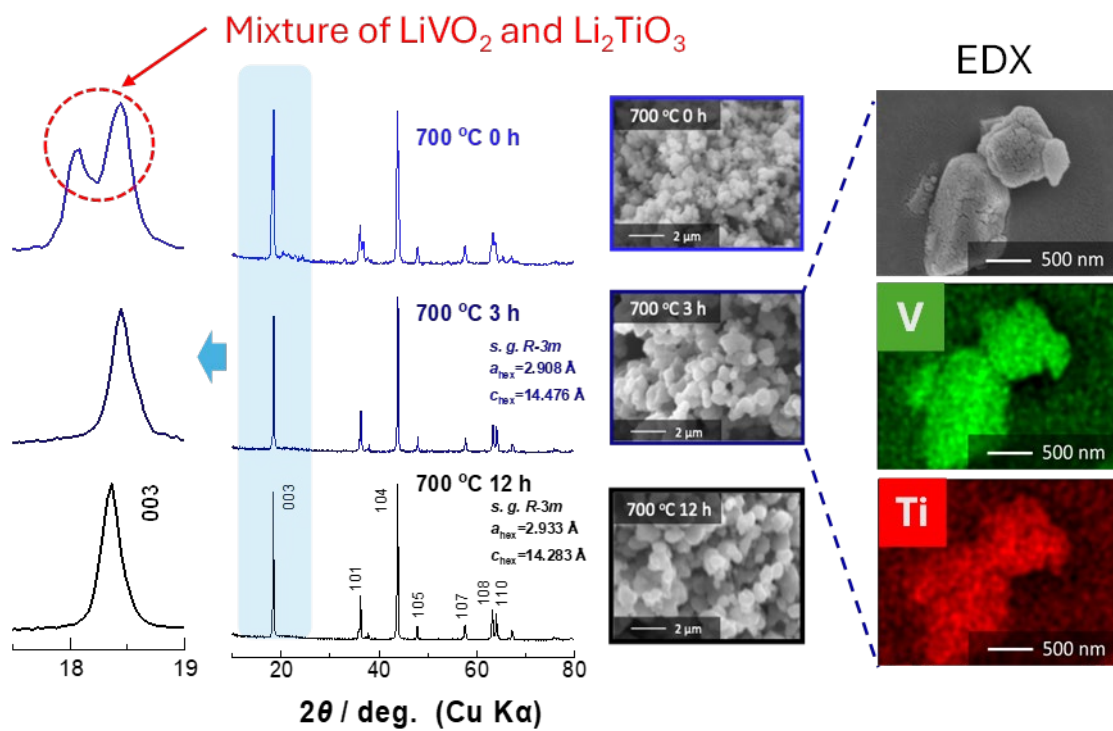


Figure S4. XRD patterns, SEM images, and EDX maps of LTVO synthesized with different calcination durations at 700 °C.

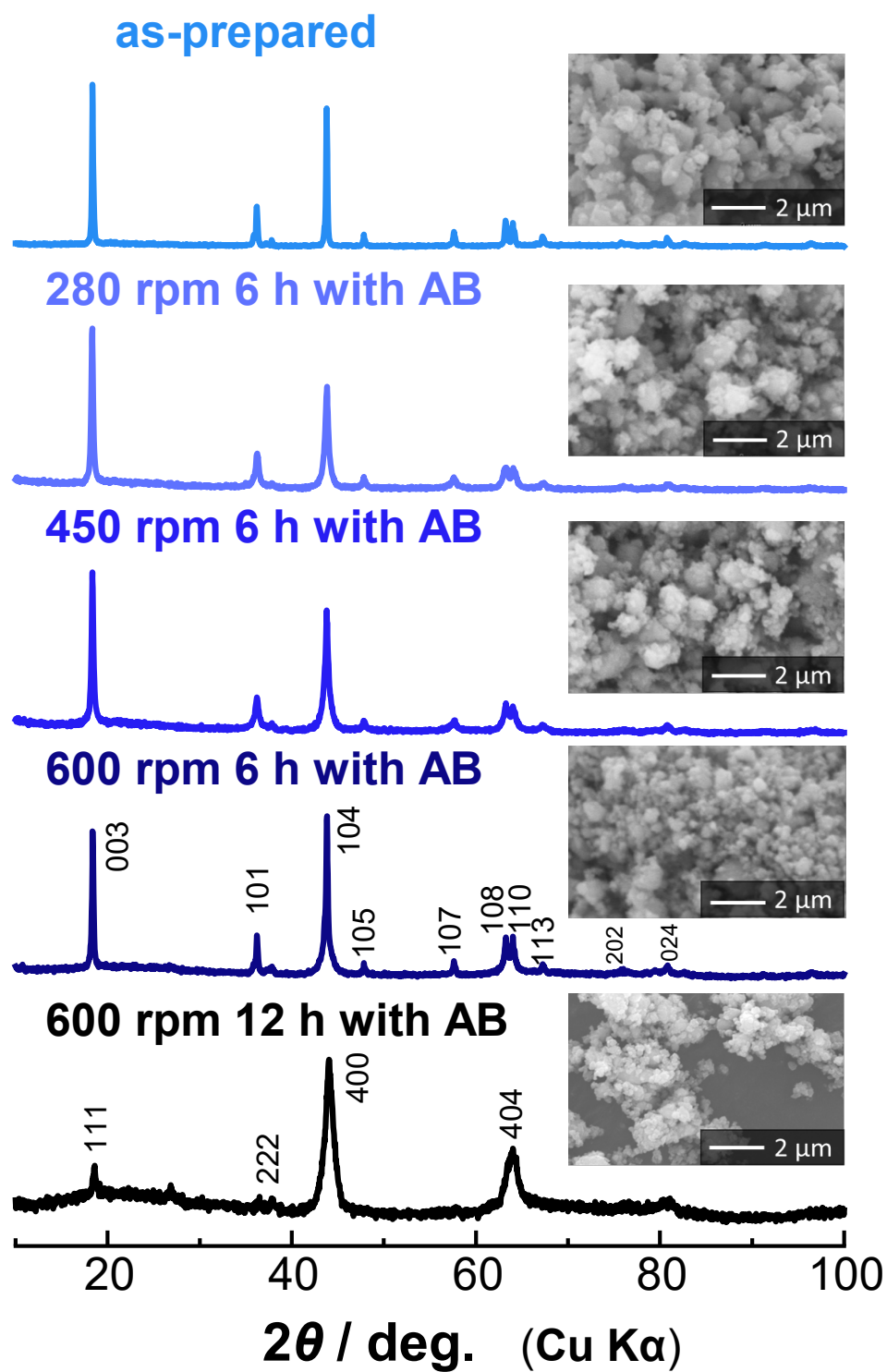


Figure S5. XRD patterns and SEM images of LTVO prepared with various ball milling conditions.

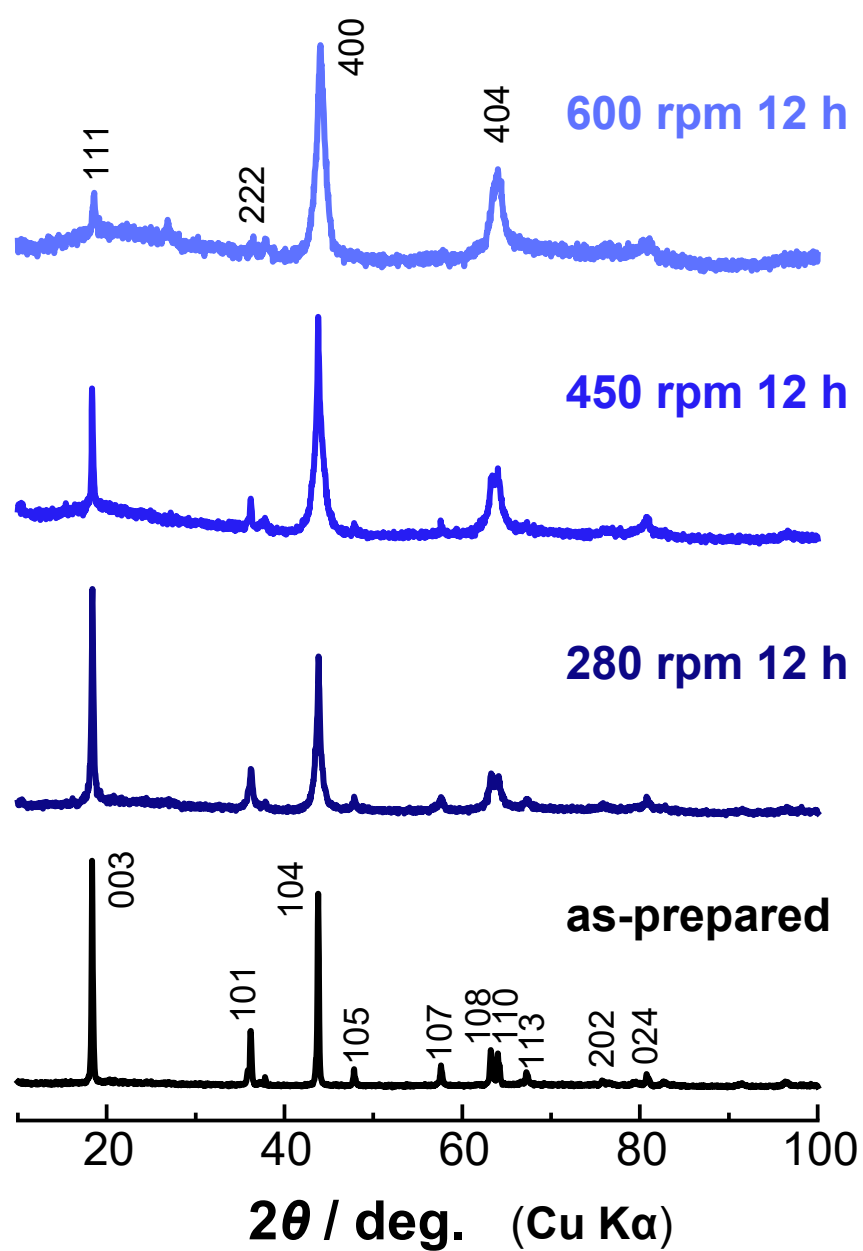


Figure S6. XRD patterns of LTVO ball-milled with various rotation speeds for 12 h.

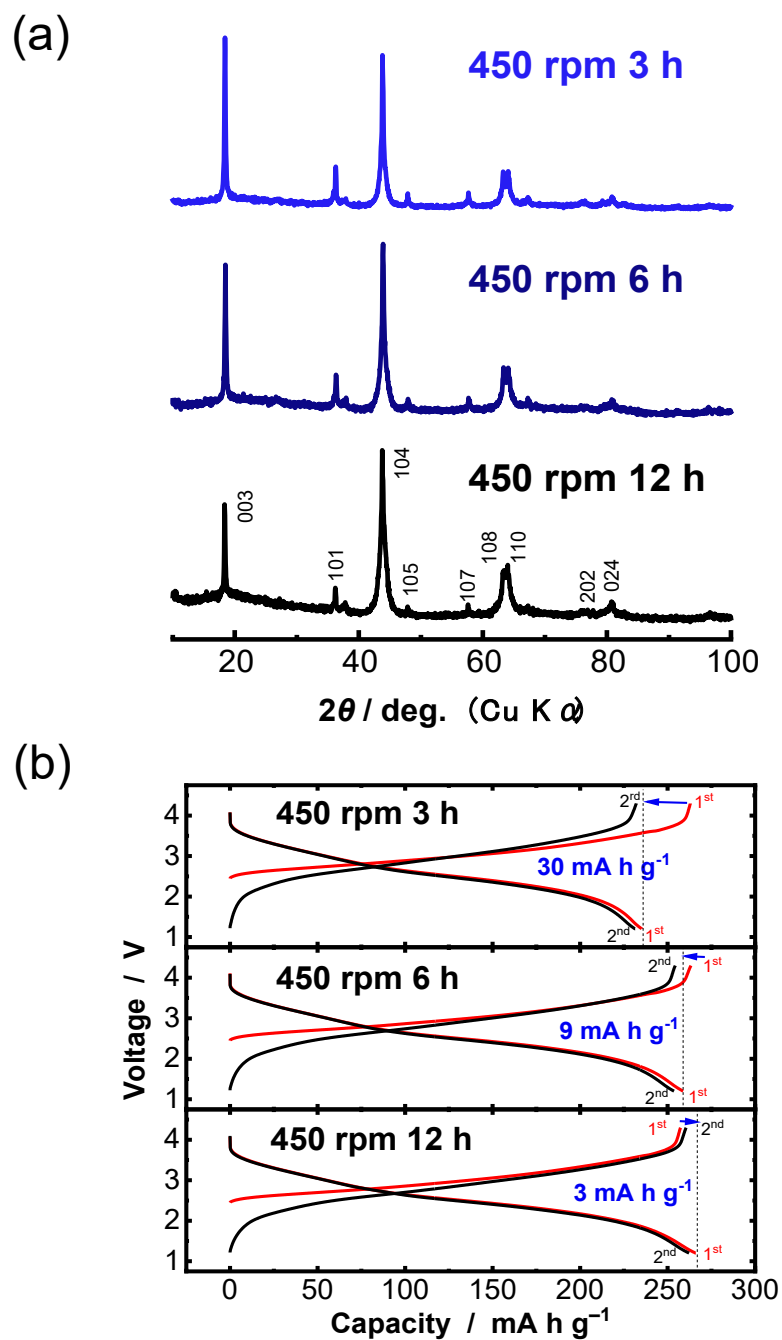


Figure S7. (a) XRD patterns and (b) galvanostatic charge/discharge curves of LTVO ball-milled with different rotation times at 450 rpm.

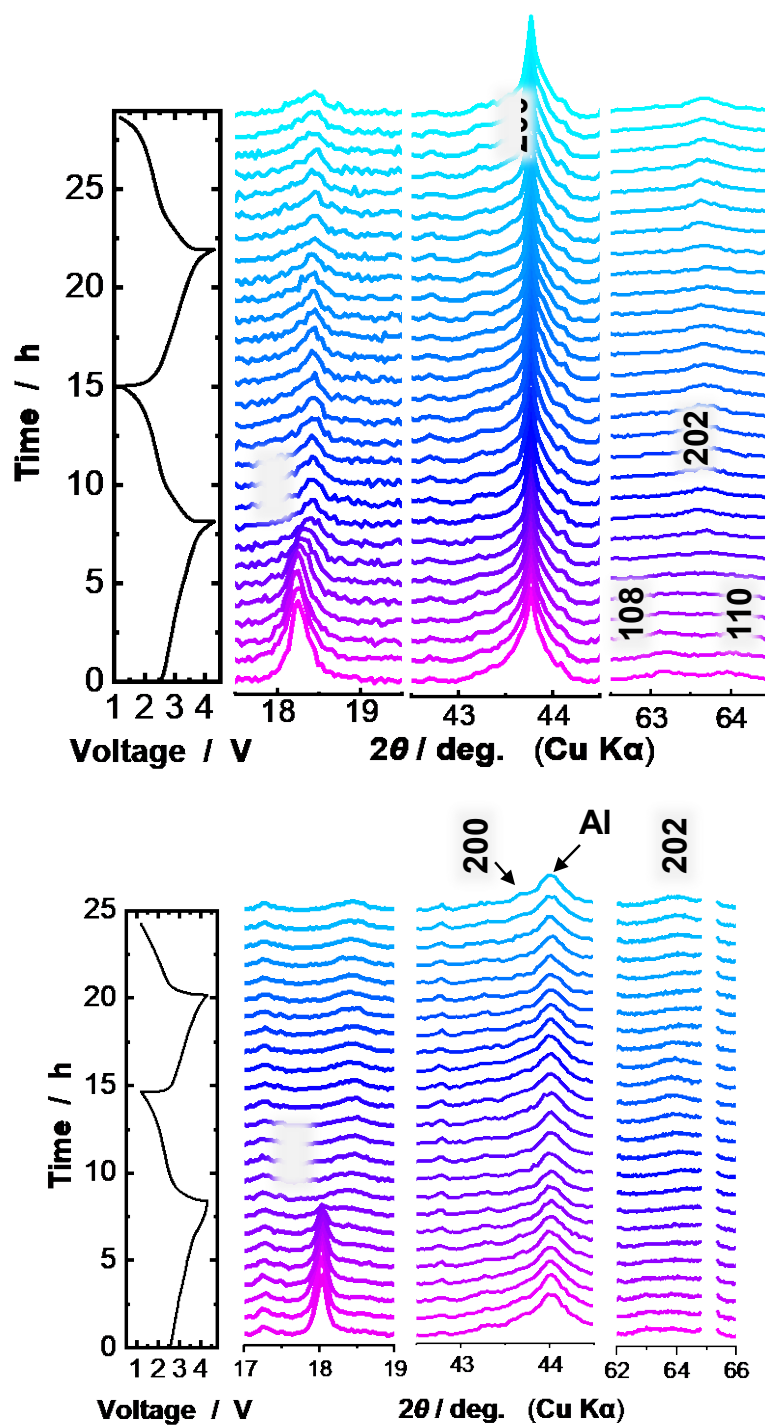


Figure S8. *In-situ* XRD patterns during charge/discharge processes at a rate of 30 mA g⁻¹ for (a) optimized LTVO and (b) LiVO₂.

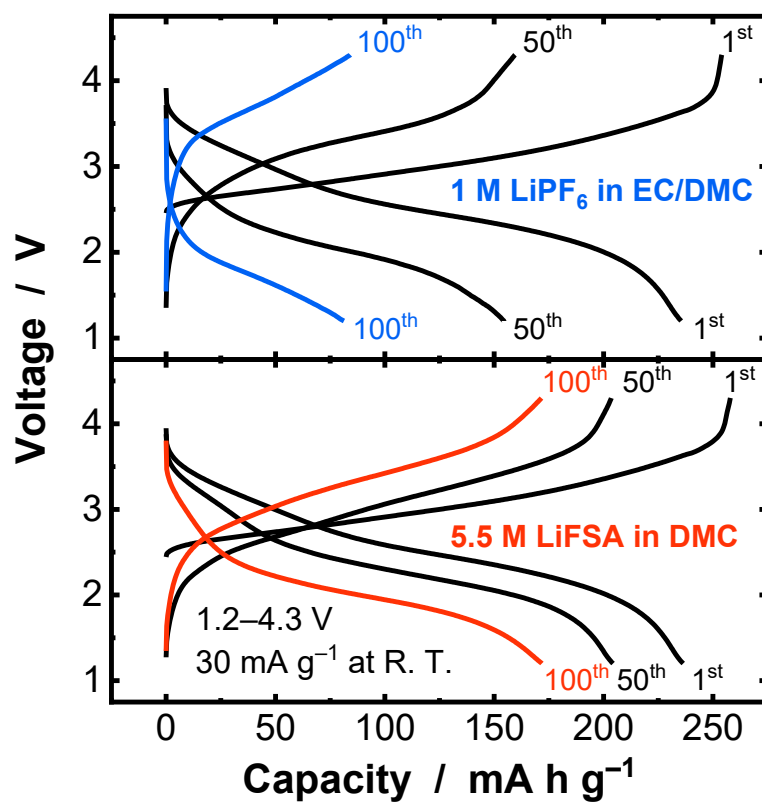


Figure S9. Galvanostatic charge/discharge curves of optimized LTVO cycled in 1.0 M LiPF_6 in EC/DMC and 5.5 M LiFSA in DMC electrolyte solutions at a rate of 30 mA g^{-1} .

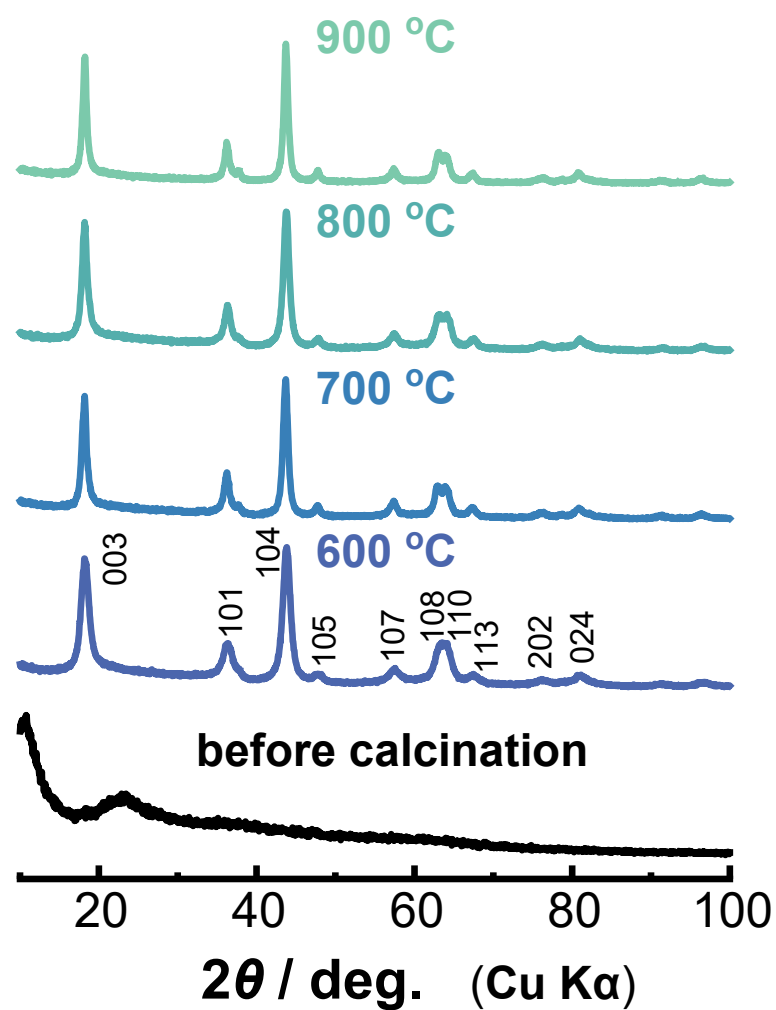


Figure S10. XRD patterns of LTVO synthesized by the solution method and calcinated at different temperatures.

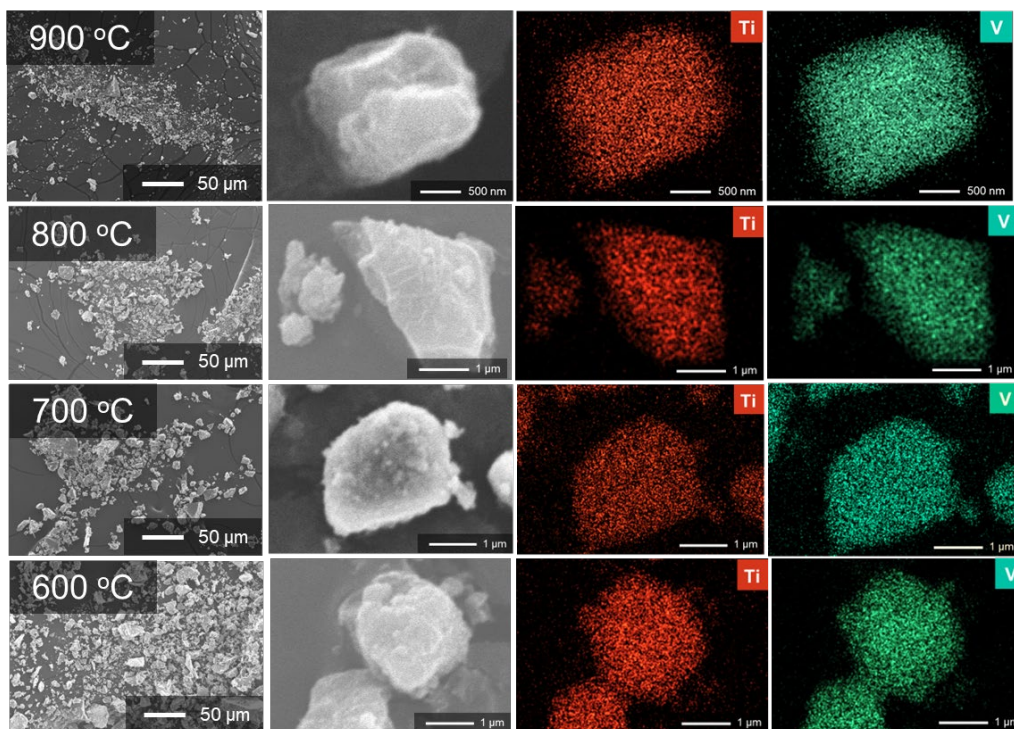


Figure S11. EDX maps of LTVO synthesized by the solution method calcinated at different temperatures.

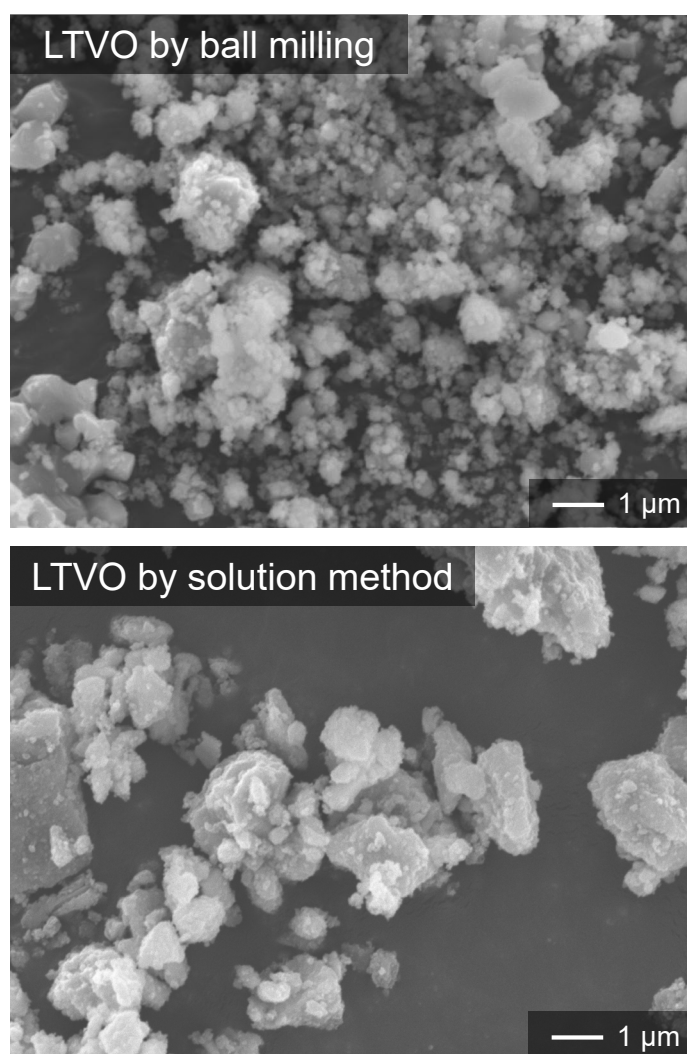


Figure S12. SEM images of LTVO synthesized by ball-milling and the solution method.

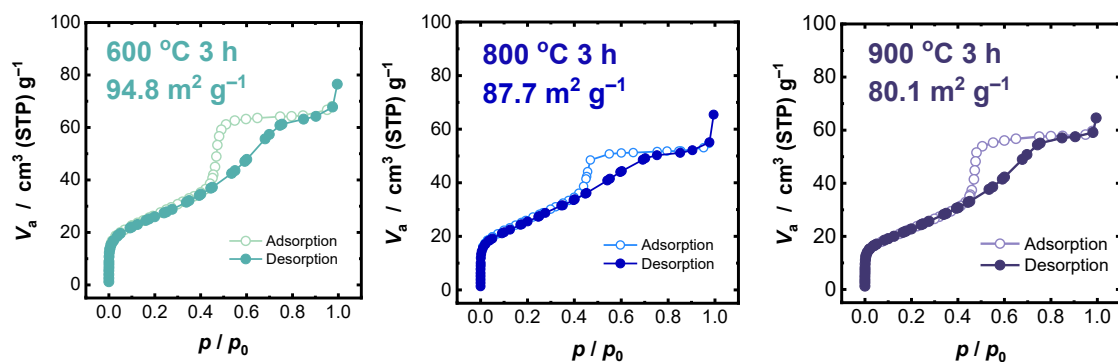


Figure S13. N_2 adsorption and desorption isotherms and corresponding BET specific surface area of LTVO synthesized by the solution method and calcinated at different temperatures.

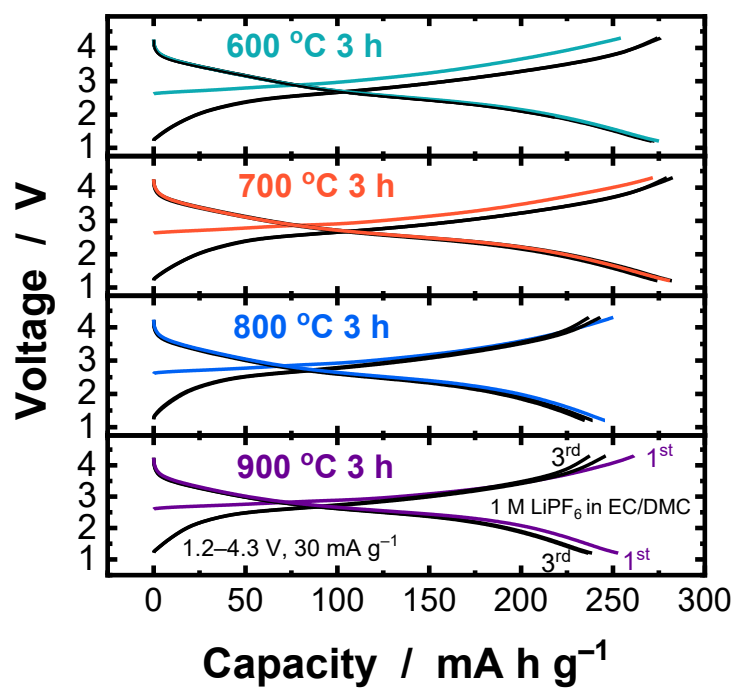


Figure S14. Galvanostatic charge/discharge curves of LTVO synthesized by the solution method and calcinated at different temperatures with 1.0 M LiPF₆ in EC/DMC at a rate of 30 mA g⁻¹.

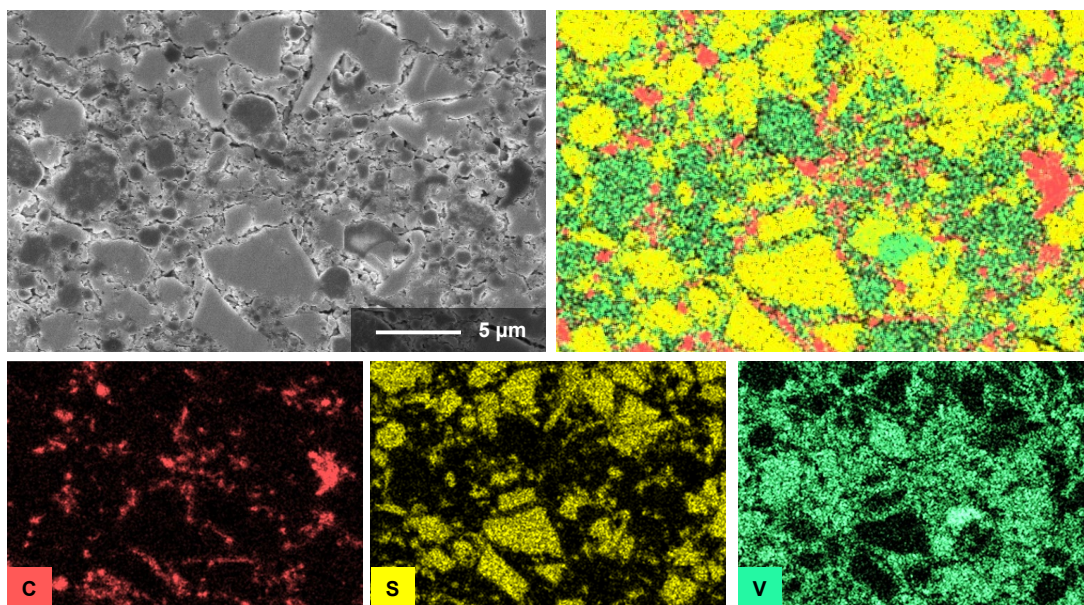


Figure S15. Cross-sectional SEM-EDX images of LTVO/LPSCI/VGCF composite electrodes with nanosized LTVO.

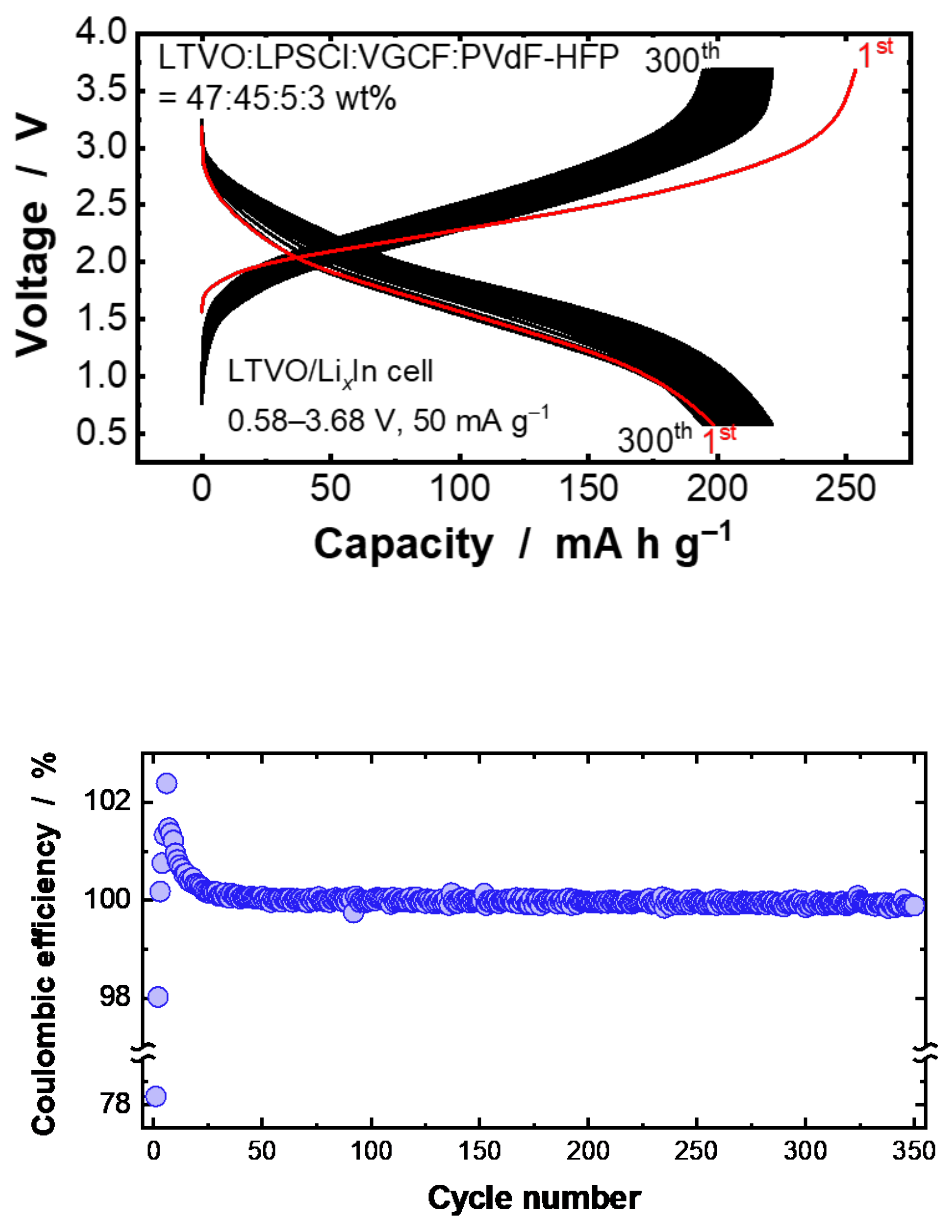
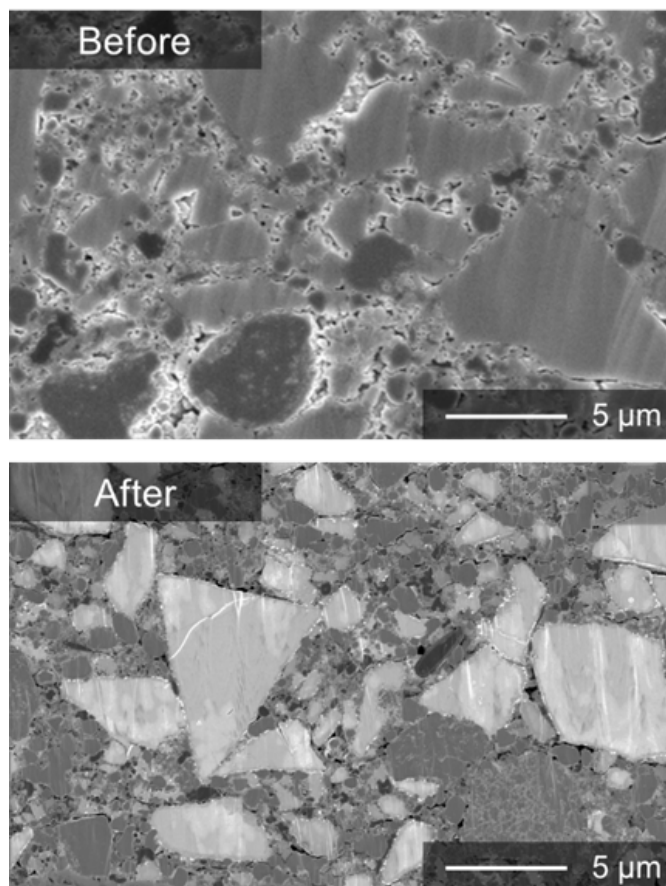


Figure S16. (a) Galvanostatic charge/discharge curves and (b) coulombic efficiency of the all-solid-state cell with optimized LTVO at a rate of 50 mA g⁻¹ at 50 °C.

(a)



(b)

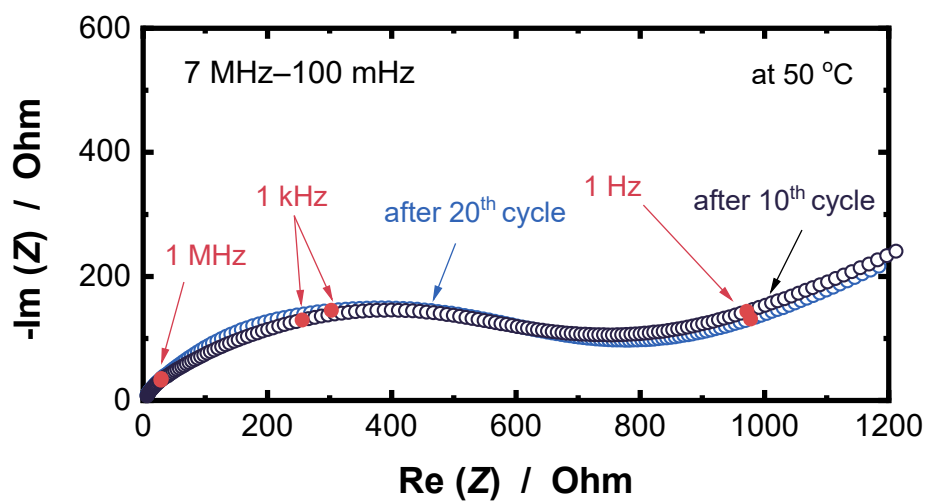


Figure S17. (a) Cross-sectional SEM images of LTVO/LPSCI/VGCF composite electrodes with optimized LTVO before and after cycling (5 cycles). (b) Nyquist plots of the all-solid-state cell after 10th and 20th cycles.

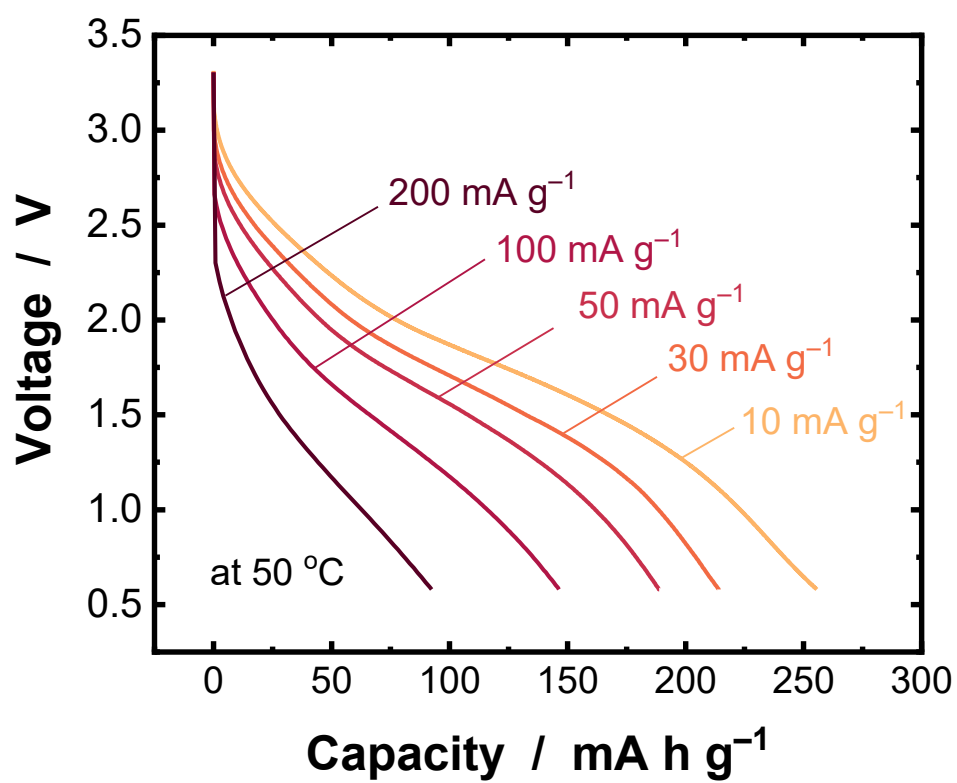


Figure S18. Rate capability of the all-solid-state cell with optimized LTVO at 50 °C with minimal stack pressure.

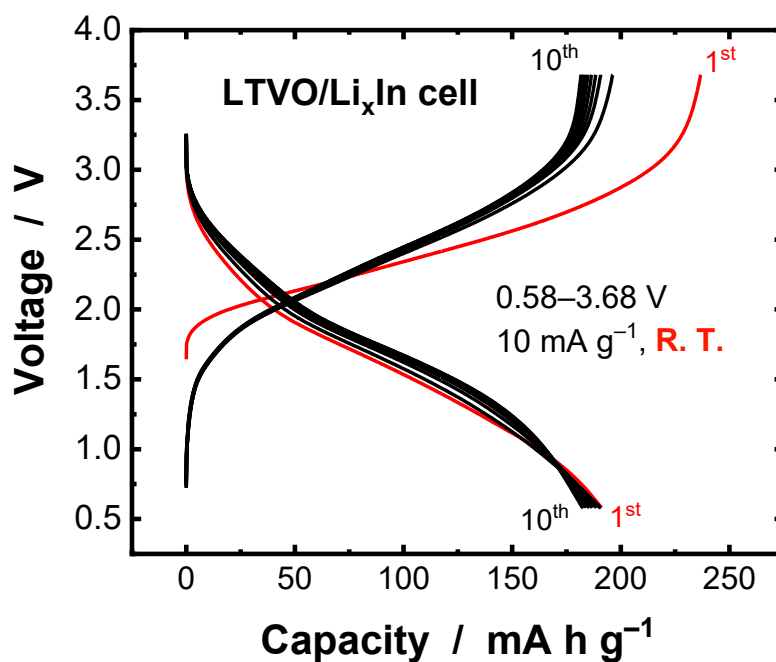


Figure S19. Charge/discharge curves of the all-solid-state cell at 10 mA g^{-1} at room temperature with minimal stack pressure.

Supplementary References

1. N. Shimada, Y. Ugata, S. Nishikawa, D. Shibata, T. Ohta and N. Yabuuchi, *Energy Advances*, 2023, **2**, 508-512.
2. Y. Ugata, C. Motoki, S. Nishikawa and N. Yabuuchi, *Energy Advances*, 2023, **2**, 503-507.
3. R. P. Rao and S. Adams, *physica status solidi (a)*, 2011, **208**, 1804-1807.
4. C. Yu, S. Ganapathy, J. Hageman, L. Van Eijck, E. R. Van Eck, L. Zhang, T. Schwietert, S. Basak, E. M. Kelder and M. Wagemaker, *ACS applied materials & interfaces*, 2018, **10**, 33296-33306.
5. J. Gao, J. Hao, Y. Gao, X. Sun, Y. Zhang, D. Song, Q. Zhao, F. Zhao, W. Si and K. Wang, *ETransportation*, 2023, **17**, 100252.
6. Y.-J. Lee, S.-B. Hong and D.-W. Kim, *Journal of Industrial and Engineering Chemistry*, 2023, **122**, 341-348.
7. J. Hwang, T. Yamamoto, A. Sakuda, K. Matsumoto and K. Miyazaki, *Electrochemistry*, 2022, **90**, 102002-102002.
8. B. D. L. Campeon, H. B. Rajendra and N. Yabuuchi, *ChemSusChem*, 2024, **17**, e202301054.